Microstructure and bending properties of solution-treated Ti-Mo binary alloys for biomedical applications

Nthabiseng Abigail Moshokoa [1, 2] , *Mampai Lerato* Raganya[1, 2], *Ronald* Machaka [1, 2], *Babatunde Abiodun* Obadele [2,3], *Mamookho Elizabeth* Makhatha[2]

[1] Advance Materials Engineering, Manufacturing Cluster, Council for Scientific and Industrial Research, Meiring Naudé Road, Brummeria, Pretoria 0184, South Africa
[2] Department of Metallurgy, School of Mining and Metallurgy and Chemical Engineering, University of Johannesburg, Doornfontein Campus, Johannesburg, South Africa
[3] Department of Chemical, Materials and Metallurgical Engineering, Botswana International University of Science and Technology, Plot 10071 Boseja, Palapye, Botswana

Abstract. The current study investigates the influence Mo on the microstructure and bending properties of solution treated Ti-xMo alloys (x= 10.00, 12.89, and 15.05 wt%). The fundamental objective of the study is to attain the correlation between the composition, processing, microstructure, and bending properties of β Ti after the solution treatment process. The alloys were fabricated using the commercially available arc melting furnace, they were subjected to solution treatment at a temperature of 1100 ℃ for 1hr and quenched in ice water. X-ray diffractometer showed peaks belonging to β and α″ phase for all the solution treated alloys, while the microstructures of all the alloys characterized by Optical microscope illustrated equiaxed β grains structure and sub-grain structures belonging to the α″ structure. The highest bending strength was found to be 1627.40 Mpa when the Mo content was 15wt%. The bending modulus decreased significantly with an increase in composition. The lowest bending modulus of 74 GPa was seen in 15.05wt% Mo alloy. The Micro-Vickers Hardness of the designed alloys increased extensively with an increase in Mo content. The fracture surfaces of the alloys after bending illustrated dimple features and pronounced cleavage facets which indicated brittle and ductile fracture in all the binary alloys.

1. Introduction

Replacement of functionally disordered hard tissue with artificial instruments such as bone plates, hip joints, spinal fixation devices, and dental roots is becoming increasingly popular [1]. Navarro et al. 2008 reported that the demand for artificial instruments made of metallic materials to substitute dysfunctional hard tissues within the population of aged groups who suffers from diseases such as arthritis and joint pains has significantly increased [2]. Metallic materials are broadly employed as biomaterials for the fabrication of orthopedic implants due

to their advantages such as superior mechanical properties which include yield strength, ductility, fatigue strength, and fracture toughness [3] and [4]. Orthopedic implants utilized for hip and knee joint replacements have high pre-requisite such as biocompatibility, low elastic modulus close to the bone, high mechanical strength to sustain long-term service period and high corrosion resistance [5]. The high pre-requisite are due to challenges such as osteoarthritis (inflammation in the bone joints), osteoporosis (weakening of the bones) and trauma that could lead to pain or loss in function of the tissue [6].

Metallic biomaterials such as Co-Cr alloys, stainless steel, and Ti6Al4V have widely been used for orthopedic implants [1] and [6]. However, stainless steel and Co-Cr alloy contain Ni and Cr respectively which causes allergies [2] and their elastic moduli are 3 times higher (240 and 210 GPa respectively) than that of the human bone (10-40 GPa) [7]. The commercially available Ti6Al4V has two disadvantages, firstly the release of V and Al ions might induce some long-term health issues [6] and [8]. For example, vanadium (V) has been found to react severely with tissue in animals, and aluminium (Al) is associated with neurological disorders and Alzheimer's disease [9]. Lastly, Ti6Al4V has a relatively higher elastic modulus (110 GPa) compared to the human bone (10-40 GPa) which causes a stress shielding effect [10]. The stress shielding effects as the insufficient load transfer from the artificial implant to the re-modeling bone which led to bone resorption and eventually loosening of the prosthetic devices [11] and [12]. Under normal circumstances, bone carries the load applied to it by itself. However, after the introduction of an implant to the bone, both the load and implants share the load. As a result, the bone expériences reduced stress [13].

Recently, many research efforts have been devoted to the study of β and metastable β Ti alloys with lower elastic modulus, better formability, and higher biocompatibility than Ti6Al4V alloys. Metastable β type Ti alloys that have been developed to date include Ti-15Mo, Ti-12Mo-6Zr-2Fe, and Ti-35Nb-7Zr-5Ta [14]. However, amongst all the developed alloys Ti-Mo and Ti-Mo-based alloys are promising alloys because Mo is an effective β stabilizer compared to other β stabilizing elements such as Nb, Ta, Zr ect. According to literature in Ti-X (X=Mo, Nb, Ta), the β is reported to be stabilized at different content for different elements, for example Mo is stabilized at 10wt% [15], Nb at 35 wt% [16], and Ta at 40 wt%[17]. Secondary phases including orthorhombic marteinsitic (α'') and omega (ω) are likely to precipitate in these alloys during cooling. Moshokoa et al 2020 investigated the influence of Mo content on the tensile properties of Ti-Mo alloys. The tensile properties were found to be strongly dependent on the phases formed, which were also obsevered to be sensitive to the Mo content in the alloy. In alloys with low Mo content, in which high proportions of the ω and/ or α'' phases were formed, the elastic moduli were higher than in alloys with higher Mo content, i.e precipitation of small proportions of the ω and/ or α'' phases results were found to be dependent on the phase constiruents formed [18]. Depending on the compositions, the omega phase and the orthohombic phases transforms during fast cooling or quenching a material from above the β transus temperature. Although, there is some published work in literature on Ti-Mo binary alloys, there is no study on the bending properties of solution treated Ti-Mo alloys for biomedical applications. Therefore, this work's objective is to study the bending properties of solution treated of Ti-xMo alloys (x= 10,02 12.89, and 15.05wt%) at room temperature.

2.Materials and Methods

2.1 Alloy Design

Three metastable β-type Ti-Mo alloys were designed using the cluster plus- glue- atom model (CPGA) and their β stabilities was predicted using the Molybdenum equivalence (Moeq), average number of valence electrons in each atom e/a ratio, and the Beta (β) stabilizing index (Kβ) concept. Their composition and β stability are presented in Table 1. The Moeq was reported by Bania et al as the expression represented the contribution of each alloying element towards β phase stability in contrast with the most effective stabilizer Mo, they reported that a Moeq of 10wt% is enough to stabilize the β phase [19]. An alloy containing a higher proportion of β stabilizers will retain 100% β phase upon quenching from the β phase region. On the contrary, secondary phases (ω and α') precipitate in the β matrix in alloys with low content of β stabilizers upon quenching from the same region. The Moeq of all the designed alloys (illustrated in table 1) were above 10wt%, which implies that the alloys will form 100% β phase.

The (e/a ratio) was used to predict the stability of the β phase. The ω phase is precipitated within the e/a ration of 4.13 and 4.30, while the 100% β phase is retained at e/a ratio above 4.30 [20]. The e/a ratio of the designed alloys were between 4.21-4.30, which indicated that the ω phase would be precipitated in the β matrix of the alloys. The K_β remains yet another approach used to determine the stability β in Ti alloys. If the K_β is in the range of 1-1.5 ($1 < K_\beta < 1.5$) then the β phase in the alloy was found to be metastable, beyond this value the β phase was found to be stable. The (K_β) of the designed alloys were found to be in the range of 1.0-1,51 and this implied that β phase was metastable.

Table 1 : Cluster Formula, Composition, Moeq, e/a ratio, and Kβ of the designed alloys

Cluster Formula	**Composition (wt%)**	**Mo(wt%)**	**Moeq (wt%)**	**e/a ratio**	**Kβ**
$[(Mo)\text{-}(Ti)_{14}]\ Ti_4$	Ti-10.02 Mo	10.02	10.02	4.20	1.00
$[(Mo)\text{-}(Ti)_{14}]\ Mo_{0.1}\ Ti_{0.9}$	Ti-12.89 Mo	12.89	12.89	4.26	1.29
$[(Mo)\text{-}(Ti)_{14}]\ Mo_{0.3}\ Ti_{0.7}$	Ti-15.05 Mo	15.05	15.05	4.30	1.51

2.2 Fabrication of Designed Alloys

The CP-Ti and Mo powders with average particle size of 28 μm and 16.83 μm (compositions shown in table 1) were compacted into green bodies using the cold press machine. The green bodies were processed using a commercially available Arc furnace, in which melting was performed under argon atmosphere in a water-cooled copper crucible. The ingots were flipped 3 times during melting for homogeneity purposes. The cast samples were solution treated using a ceramic furnace at 1100 ℃ for 1 h and subsequently quenched in ice water. The compacted green body and solution treated ingot are illustrated in figure 1 (a) and (b) respectively.

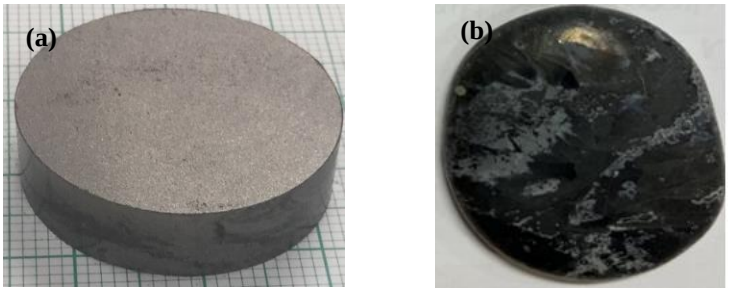

Figure 1 : Typical Ti-Mo (a) Compacted green body and (b) Solution treated ingot.

2.3 Microstructural Characterization

The phase and the microstructures of solution treated specimens were studied using an X-ray diffractometer (XRD), and the Optical microscope (OM). The OM samples were prepared following standard metallographic procedures and subsequently etched in Kroll reagent for 30 seconds. The samples were analyzed for microstructure using the Leica microscope.

2.4 Mechanical Properties

A 3-point bend test was carried out using an Instron^{TM}1342 testing machine. The bending strength of the studied alloys was determined according to ASTM : D790-03. The equation of the bending /flexural strength is given as.

$$\sigma_f = 3PL/2bw_2 \qquad (1)$$

Where σ_f is the bending strength (MPa), P is the load (N) of 1725.47N, L is the span length (mm), b is the specimen width (mm) and w is the thickness of the specimen (mm). The dimensions of the specimens were : L= 30 mm, b=4.0 mm, and w=3.0mm. The average bending strength was taken from at least 3 specimens under the same conditions (testing temperature of 20ºC and testing rate of 2.0 mm/min). The bending modulus of the designed alloys was calculated using the following formula

$$E = L^3 \Delta P/4bh^3\Delta\delta \qquad (2)$$

Where E is the elastic bending modulus (GPa), ΔP is the load increment as measured from the preload (N), L is the span length (mm), b is the specimen width (mm), and h is the thickness of the specimen and Δδ is the deflection increment at midspan as measured from the preload. The Micro-Vickers hardness of the designed alloys was measured using the Zwick Roell Vickers hardness tester. Zwick Roell Vickers hardness tester under load of 500 gf and dwell time of 10 s. The presented microhardness values are measures of 10 indentations per sample and their average values were calaculated.

3. Experimental Results

3.1 Phase and Microstructural Characterization

3.1.1 X-ray diffraction

X-ray diffraction (XRD) was conducted to identify the constituent phases of the solution-treated Ti-Mo alloys. The XRD patterns are illustrated in Figure . The XRD patterns of Ti-10.02wt% Mo, exhibits peaks corresponding to the orthorhombic martensitic α″ phase peaks and bcc β phase peaks. The XRD pattern of Ti-12.89wt% Mo and Ti-15.05wt% Mo illustrated only bcc β phase. There was no evidence of new transformed peaks such as the α″ or ω phases on the solution treated alloys after solution treatment. As the Mo content increases, the formation of the α″ phase decreased significantly leading to stabilization of the bcc β phase. The XRD results of the solution treated Ti-10.02wt% Mo and Ti-15.05wt% Mo alloys were in agreement with the results reported by [21] , [22] and [23].

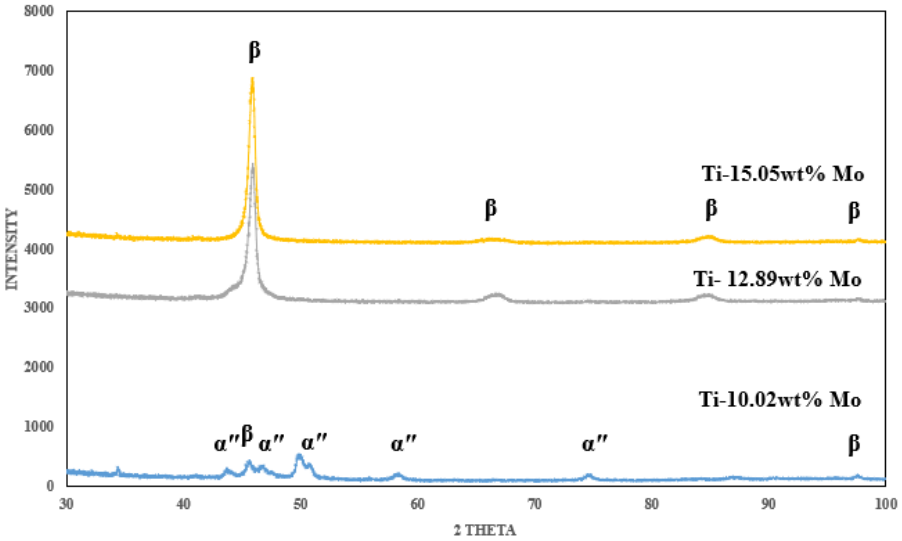

Figure 2 : X-ray diffraction of Ti-xMo (x-10.02, 12.89 and 15.05wt%) alloys.

3.1.2 Optical Microscope

The optical micrographs (OM) of the solution treated Ti-Mo alloys is depicted in Figure . The OM micrographs of 10.02wt% Mo-alloy were comprised large equiaxed grains of β structure and acicular sub-grain structures precipitated inside the grains. The morphology of the sub-grain structure were established to be corresponding to orthorhombic martensitic structure (α″). Similar results were reported by Davis et al [24] in Ti-6wt% Mo alloys. As the Mo content increased to Ti-12.89wt% Mo and Ti-15.05wt% Mo, the OM micrographs showed only the equiaxed grains of β structure only. There were no signs of sub-grain structures belonging to the orthorhombic martensitic structure (α″) and this implies that the martensitic start temperature was below temperature during quenching/cooling. The micrographs analyzed using the OM technique in 10.02wt% Mo were found to be in accord with those presented by [22] but contradicting the ones reported by [21]. However, the Ti-15.05wt% Mo alloy was consistent with experimental results reported by [21]–[23].

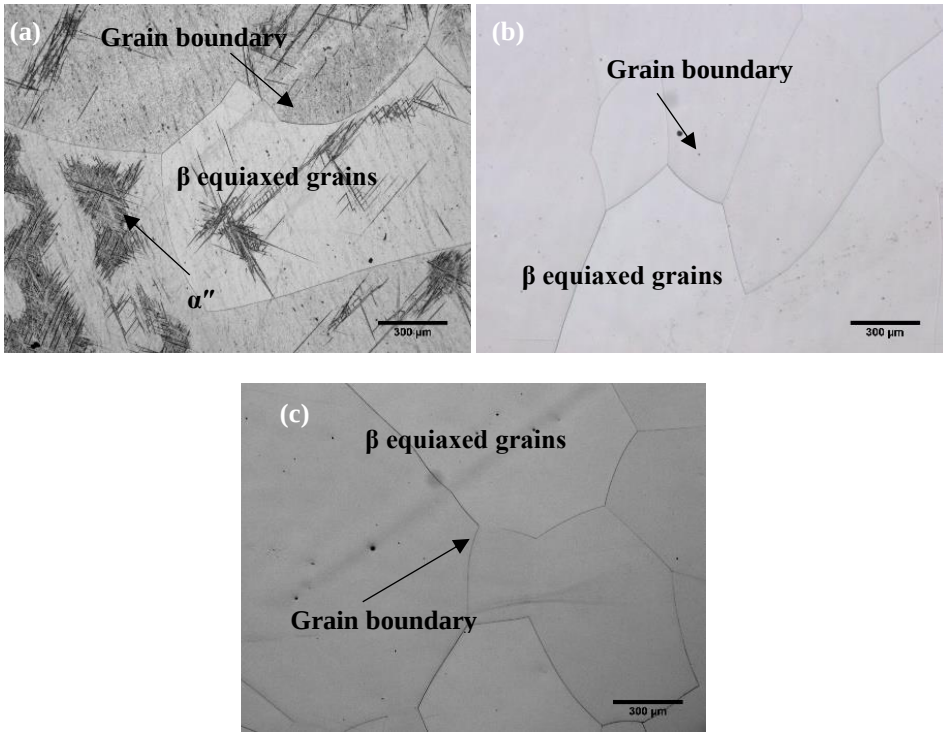

Figure 3: OM micrographs of Ti-Mo alloys : (a) Ti-10.02wt% Mo, (b) Ti-12.89wt% Mo and (c) Ti-15.05wt% Mo.

It is noteworthy that the ω phase could have precipitated during cooling in all the alloys. However, the detection of this phase using the conventional XRD and OM techniques is rendered challenging due to the low intensity of its peaks. From literature the ω phase was detected in Ti-10wt% Mo [25], in Ti-12wt% Mo [26], in Ti-15wt% Mo [27] using the Transmission electron microscopy (TEM) technique and in Ti-15Mo [28] using the syncronton XRD. Segregation of Mo tends to occur in Ti alloys during solidification, resulting in Mo rich and Mo lean regions [29] and [30]. In Mo rich regions the β phase is more stable while the precipitation of the ω phase is suppressed. On the contrary in Mo lean regions the stability of the β phase is lower , while the formation of the ω phase is greater.

Table 2 compares the theoretical findings with the experimental findings of the designed alloys. The experimental results of the designed alloys analyzed by the XRD and OM techniques for Ti-10.02wt% Mo alloys were found to be inconsistent with the theoretical findings due to the orthorhombic martensitic α″ phase observered experimentally. However, the experimentally obtained results in Ti-12.89wt% Mo and Ti-15.05wt% Mo alloys corraborated with the predictions methods (Moeq, Kβ, and e/a ratio).

Table 2 : Theoretical Findings vs Experimental Findings of Ti-Mo alloys

	Theoretical Findings			**Experimental findings**	
Mo Content (wt. %)	**Moeq (wt. %)**	**K_β**	**e/a ratio**	**XRD**	**OM**
Ti-10.02 Mo	β	β	β	**β+α″**	**β+α″**
Ti-12.89 Mo	β	β	β	**β**	**β**
Ti-15.05 Mo	β	β	β	**β**	**β**

3.2 Mechanical Properties

3.2.1 Bending Strength

Ideal biomedical materials must have high bending strength to sustain the load bearing function of human bone and reconstruction. The bending strength of the quenched Ti-Mo alloys are presented in Figure . The measured bending strength of Ti-10.02wt% Mo was 1552.30 MPa. When the Mo content increased to Ti-12.89wt% Mo, no significant change in the bending strength was observerd. When the Mo content increased to 15.05wt% the bending strength increased significantly to 1627.40Mpa. The significant change observed in Ti-15.05wt% Mo could be attributed to the tentative presence of the ω phase as a result of segregation, which leds to its precipitation in potetial Mo-lean regions in the alloy. In metastable β alloy, the ω phase tend to increase the strength of the alloys [31]. The α"phase is reported to have higher strength compared to the β phase [32]. The bending strengths of Ti-10.02wt% Mo and Ti-12.89wt% Mo alloys are lower but the 15.05wt% Mo alloy is higher as compared to the ones reported by [33] in as-cast conditions (1752 MPa in Ti-10wt% Mo, 1440 MPa in Ti-12.89wt% Mo and 1348 MPa in Ti-15wt% Mo).The highest bending strength of 1627.4 MPa in Ti-15.05wt% Mo illustrates the potential of being used in biomedical applications as compared to the bending sgrength of commercially available Titanium (Cp-Ti) of 844.00 Mpa [34] and 900Mpa [35].

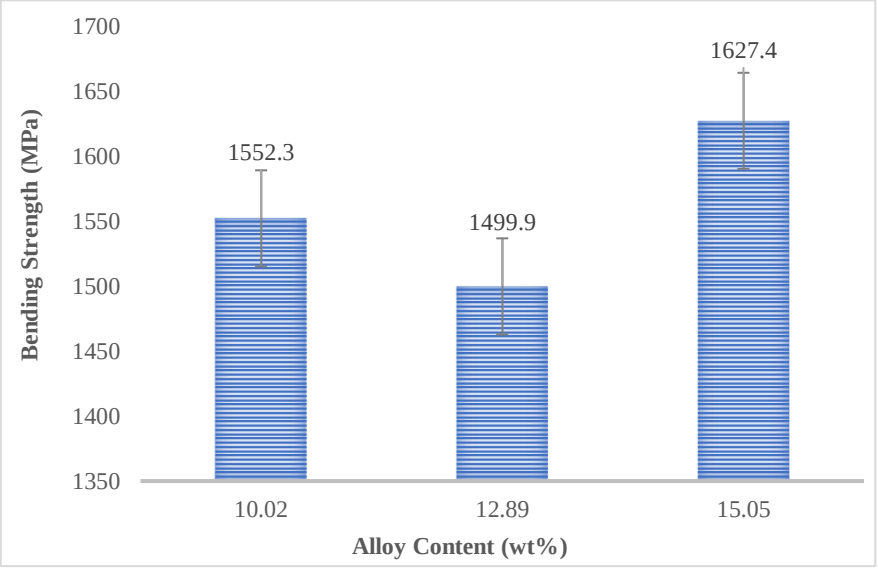

Figure 4: Bending Strength of binary Ti-Mo alloys

3.2.2 Bending Modulus

The bending modulus of the designed binary Ti-Mo alloys is presented in Figure . The bending modulus were calculated using equation 2 as stated in the material and methods section.. The Ti-10.02wt% Mo-alloy illustrated the highest bending modulus of 97GPa. When the Mo contnet increased to Ti-12.89wt% Mo the bending modulus decreased extensively to 84GPa. Further increase in the Mo content to Ti-15.05wt% Mo the bending

modulus decreased significantly to 74GPa.The bending modulus showed a decrease with an increase in Mo content. The phases in metastable β Ti type influence the modulus in the following : $E_{\omega} > E_{\alpha'} > E_{\alpha''} > E_{\beta}$ [36]. The α" and the ω phase possess high moduli compared to the β phase [37]. The bending modulus in Ti-10.02wt% Mo could be attributed to the presence of α" depicted in the XRD pattern and the OM micrograph. Furthermore, the tentative presence of the ω phase, which is more effective in increasing the modulus, could have contributed to the highest bending modulus value of the alloy. Th influence of Mo segregation on mechanical properties can be observerd where regions with lower Mo content corresponds to higher value of bending modulus [29]. The bending moduli of the studied alloys was found to be lower than that of the commercially pure Ti (CP-Ti) of (99 GPa) [38]. The lowest bending modulus in Ti-15.05wt% Mo demonstrated its potential to be used as implant material and prevent the stress shielding effect to occur.

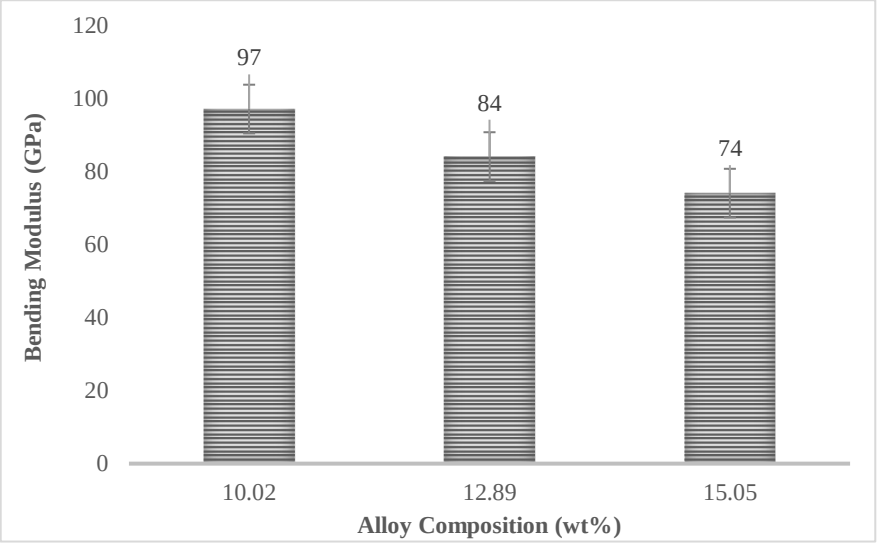

Figure 5: Bending Modulus of binary Ti-Mo alloys

3.2.3 Fracture surfaces of Ti-Mo alloys after 3-point Bend Test

The fracture surfaces analyzed using the SEM technique are illustrated in Figure . The Ti-10.02wt% Mo showed small dimple features and more pronounced cleavage facets this implied that the alloys exhibited both brittle fracture and ductile fracture. The presence of both fractures in this alloy could be attributed to the presence of the ω phase in addition to the β and α" phase. The presence of the ω may be attributed to the segregation that occured in Mo-lean alloys. When the Mo content increased to Ti-12.89wt% Mo and Ti-15.05wt% Mo, the fracture surfaces were composed more cleavage facets as compared to dimple fracture and this implied that the alloy experienced brittle fracture more than ductile fracture. The unexpected fracture surfaces in the Ti-12.89wt% Mo and Ti-15.05wt% Mo alloys with dominant β phase as seen in the XRD patterns may be attributed by the tentative presence of the ω phase which is a brittle phase compared with the β phase.

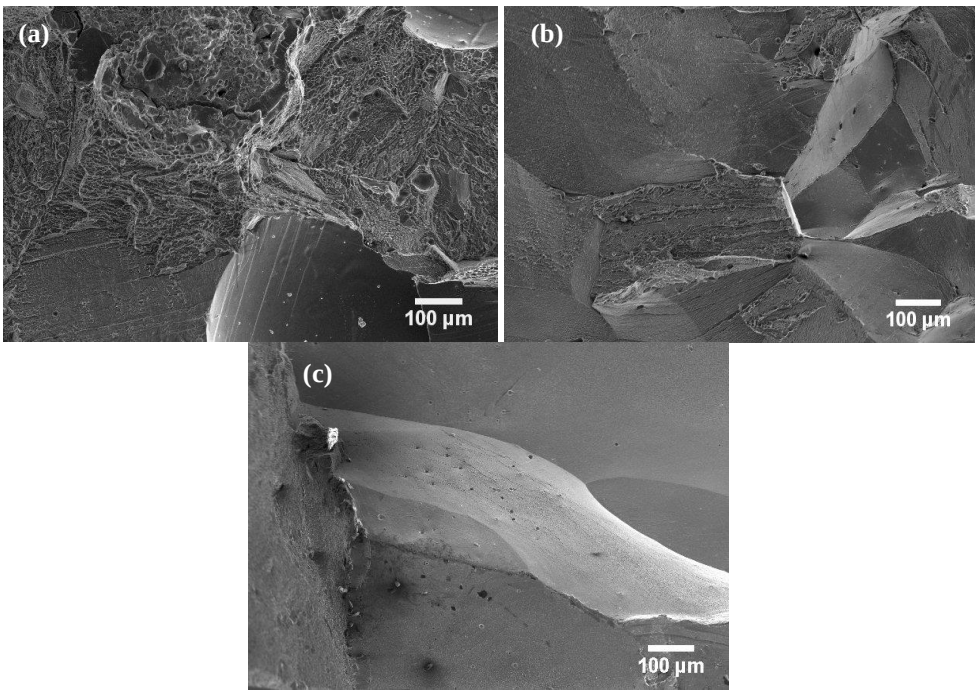

Figure 6: Fracture surface micrographs of the binary Ti-Mo alloys : (a) Ti-10.02wt% Mo, (b) Ti-12.89wt% Mo and (c) Ti-15.05wt% Mo.

3.2.4 Micro-Vickers Hardness

The Micro-Vickers microhardness of the alloys are presented in Table 3. The Ti-10.02wt% Mo show the lowest hardness of 333.5 $HV_{0.5}$. As the Mo content increased to Ti-12.89wt%, the micro-hardness increased to (335.5 $HV_{0.5}$). Further increase in the Mo content to Ti-15.05wt% the micro-hardness increased significantly to 354.5 $HV_{0.5}$. The phase constituent affects the Vickers micro-hardness value of β Ti alloys in the following manner as; $H_{\omega} > H_{\alpha'} > H_{\alpha''} > H_{\beta} > Hv_{\alpha}$ [36]. It is illustrated that the micro-hardness increased as the Mo content increased. Similar to the bending strengths and moduli of the alloys, the tentative precipitation of the undesirable ω phase could have led to the increasing micro-hardness values with increasing Mo content. The micro-hardness values of the investigated alloys were found to be higher than that of Cp-Ti and Ti-10Mo, as shown in Table 3. Moreover, the obtained micro-hardness values in Ti-- 0.02wt%Mo and Ti-15.05wt%Mo (298 and 340 $HV_{0.5}$ respectively) alloys were higher than the values measured by reaserchers in Ref [21].

Table 3: Micro-Vickers Hardness values of Ti-Mo alloys.

Alloy Content (wt%)	**Vickers Microhardness ($HV_{0.5}$)**	**Reference**
Ti-10.02wt% Mo	333.5	This Study
Ti-12.89wt% Mo	335.5	This Study
Ti-15.05wt5 Mo	354.6	This Study
Cp-Ti	190	[35]
Ti-10 Mo	298	[21]

Ti-15 Mo	340	[21]

4. Conclusions

Based on the effect of Mo on the microstructural and mechanical properties of solution treated Ti-Mo binary alloys the following assumptions could be drawn :

- XRD diffractions of the designed alloy Ti-10.02wt%Mo showed both β and α" phase peaks and the Ti-12.89wt%Mo and Ti-15.05wt%Mo alloys showed only β phase. The OM images of the alloys exhibited equiaxed β grains only.
- The XRD and OM results of Ti-10.02wt% Mo alloy were found to be inconsistent with the theoretically predicted results. Conversely, the experimental findings of Ti-12.89wt% Mo and Ti-15.05wt% Mo alloys were consistent with the theoretical predictions.
- The bending moduli of alloys decreased significantly with an increase in Mo content. The Micro-Vickers hardness of the designed alloys increased notably with an increase in the Mo content.
- The fracture surfaces of the designed Ti-10.02wt% Mo showed both dimples and cleavage facets, indicating both brittle and ductile fracture. Whereas the Ti-12.89wt% Mo and Ti-15.05wt% Mo showed more cleavage facets with less dimple. This indicated that the alloys experience more brittle fracture and less ductile fracture.
- The tentative precipitation of the ω phase could have occurred greatly in regions lean in Mo, due to segregation. The unexpected findings observed in this study are attributable to the presence of this phase in the alloys.

5. Acknowledgement

I would like to acknowledge the NRF (Thuthuka GRANT No : 115859) for funding this project, the CSIR, Mintek, and UP for their laboratory access. Gratitude to Dr. Babatunde Abiodun Obadele, Dr. Lerato Raganya, Prof. Ronald Machaka, and Prof. Elizabeth Makhatha for their supervision.

6. References

[1] M. Niinomi, S. Technol, A. Mater, and M. Niinomi, “Advanced Materials Related content Recent research and development in titanium alloys for biomedical applications and healthcare goods Recent research and development in titanium alloys for biomedical applications and healthcare goods,” 2003, doi: 10.1016/j.stam.2003.09.002.

[2] M. Navarro, A. Michiardi, and O. Castan, “Biomaterials in orthopaedics,” no. January 2014, 2008, doi: 10.1098/rsif.2008.0151.

[3] Y. Okazaki and E. Gotoh, “Comparison of metal release from various metallic biomaterials in vitro,” vol. 26, pp. 11–21, 2005, doi: 10.1016/j.biomaterials.2004.02.005.

[4] V. I. Sikavitsas, J. S. Temeno, and A. G. Mikos, “Biomaterials and bone mechanotransduction,” vol. 22, pp. 2581–2593, 2001.

[5] S. S. Sidhu, H. Singh, and M. A. H. Gepreel, “A review on alloy design, biological response, and strengthening of β-titanium alloys as biomaterials,” *Mater. Sci. Eng.*

C, vol. 121, no. October 2020, p. 111661, 2021, doi: 10.1016/j.msec.2020.111661.

[6] M. Long and H. J. Rack, "Titanium alloys in total joint replacement — a materials science perspective," vol. 19, 1998.

[7] Q. Chen and G. A. Thouas, "Metallic implant biomaterials," *Mater. Sci. Eng. R Reports*, vol. 87, pp. 1–57, 2015, doi: 10.1016/j.mser.2014.10.001.

[8] J. Lu, Y. Zhao, P. Ge, and H. Niu, "ScienceDirect Microstructure and beta grain growth behavior of Ti – Mo alloys solution treated," *Mater. Charact.*, vol. 84, no. 96, pp. 105–111, 2013, doi: 10.1016/j.matchar.2013.07.014.

[9] S. Yumoto *et al.*, "aluminum neurotoxicity in the rat brain," *Int. J. Pixe*, vol. 02, no. 04, 1992, doi: https://doi.org/10.1142/S0129083592000531.

[10] D. R. Sumner, T. M. Turner, R. Igloria, R. M. Urban, and J. O. Galante, "Functional adaptation and ingrowth of bone vary as a function of hip implant stiffness," vol. 31, 1998.

[11] Z. K. Liu, H. Zhang, S. Ganeshan, Y. Wang, and S. N. Mathaudhu, "Computational modeling of effects of alloying elements on elastic coefficients," *Scr. Mater.*, vol. 63, no. 7, pp. 686–691, 2010, doi: 10.1016/j.scriptamat.2010.03.049.

[12] B. J. Engh CA, "The influence of stem size and extent of porous coating on femoral bone resorption after primary cementless hip arthroplasty.," vol. 231, pp. 7–28, 1988.

[13] H. Weinans, R. Huiskes, and H. J. Grootenboer, "The behavior of adaptive bone-remodeling simulation models," *J. Biomech.*, vol. 25, no. 12, pp. 1425–1441, 1992, doi: 10.1016/0021-9290(92)90056-7.

[14] R. Banerjee, S. Nag, J. Stechschulte, and H. L. Fraser, "Strengthening mechanisms in Ti–Nb–Zr–Ta and Ti–Mo–Zr–Fe orthopaedic alloys," *Biomaterials*, vol. 25, no. 17, pp. 3413–3419, 2004.

[15] W. F. Ho, S. C. Wu, S. K. Hsu, Y. C. Li, and H. C. Hsu, "Effects of molybdenum content on the structure and mechanical properties of as-cast Ti-10Zr-based alloys for biomedical applications," *Mater. Sci. Eng. C*, 2012.

[16] Y. L. Hao *et al.*, "Young ' s Modulus and Mechanical Properties of Ti-29Nb- 13Ta-4 . 6Zr in Relation to ␣ Jb Martensite," vol. 33, no. October, pp. 3137–3144, 2002.

[17] W. Weng, A. Biesiekierski, Y. Li, and C. Wen, "Materialia Effects of selected metallic and interstitial elements on the microstructure and mechanical properties of beta titanium alloys for orthopedic applications," vol. 6, no. February, 2019, doi: 10.1016/j.mtla.2019.100323.

[18] N. Moshokoa, L. Raganya, B. A. Obadele, R. Machaka, and M. E. Makhatha, "Microstructural and mechanical properties of Ti-Mo alloys designed by the cluster plus glue atom model for biomedical application," *Int. J. Adv. Manuf. Technol.*, 2020, doi: 10.1007/s00170-020-06208-7.

[19] P. J. Bania and W. M. Parris, "High strength alpha-beta titanium-base alloy." Google Patents, Jul. 24, 1990.

[20] H. Ikehata, N. Nagasako, T. Furuta, A. Fukumoto, K. Miwa, and T. Saito, "First-principles calculations for development of low elastic modulus Ti alloys," *Phys. Rev. B*, vol. 70, no. 17, p. 174113, 2004.

[21] F. F. Cardoso, P. L. Ferrandini, E. S. N. Lopes, A. Cremasco, and R. Caram, "Ti – Mo alloys employed as biomaterials : Effects of composition and aging heat treatment on microstructure and mechanical behavior," *J. Mech. Behav. Biomed. Mater.*, vol. 32, pp. 31–38, 2014, doi: 10.1016/j.jmbbm.2013.11.021.

[22] C. H. Wang *et al.*, "Martensitic microstructures and mechanical properties of as-quenched metastable b -type Ti – Mo alloys," pp. 6886–6896, 2016, doi: 10.1007/s10853-016-9976-6.

[23] X. Zhao, M. Niinomi, M. Nakai, and J. Hieda, "Acta Biomaterialia Beta type Ti – Mo alloys with changeable Young ' s modulus for spinal fixation applications," *Acta*

Biomater., vol. 8, no. 5, pp. 1990–1997, 2012, doi: 10.1016/j.actbio.2012.02.004.
[24] R. Davis, H. M. Flower, and D. R. F. West, "Martensitic transformations in Ti-Mo alloys," *J. Mater. Sci.*, vol. 14, no. 3, pp. 712–722, 1979, doi: 10.1007/BF00772735.
[25] Y. L. Zhou and D. M. Luo, "Microstructures and mechanical properties of Ti-Mo alloys cold-rolled and heat treated," *Mater. Charact.*, vol. 62, no. 10, pp. 931–937, 2011, doi: 10.1016/j.matchar.2011.07.010.
[26] F. Sun, F. Prima, and T. Gloriant, "High-strength nanostructured Ti – 12Mo alloy from ductile metastable beta state precursor," *Mater. Sci. Eng. A*, vol. 527, no. 16–17, pp. 4262–4269, 2010, doi: 10.1016/j.msea.2010.03.044.
[27] J. M. Bennett, "Strengthening of metastable beta titanium alloys," no. October, 2018.
[28] M. Sabeena, A. George, S. Murugesan, R. Divakar, E. Mohandas, and M. Vijayalakshmi, "Microstructural characterization of transformation products of bcc b in Ti-15 Mo alloy," *J. Alloys Compd.*, vol. 658, pp. 301–315, 2016, doi: 10.1016/j.jallcom.2015.10.200.
[29] J. Ruzic, S. Emura, X. Ji, and I. Watanabe, "Materials Science & Engineering A Mo segregation and distribution in Ti – Mo alloy investigated using nanoindentation," *Mater. Sci. Eng. A*, vol. 718, no. July 2017, pp. 48–55, 2018, doi: 10.1016/j.msea.2018.01.098.
[30] J. Gao *et al.*, "Segregation mediated heterogeneous structure in a metastable β titanium alloy with a superior combination of strength and ductility," *Sci. Rep.*, no. April, pp. 1–11, 2018, doi: 10.1038/s41598-018-25899-3.
[31] R. Graft WH, DW lEVINSON, "The influence of alloying on the elastic modulus of titanium alloys," *Trans. Nonferrous Met. Soc. China*, 1957.
[32] Y. T. Lee, M. Peters, and G. Wirth, "Effects of thermomechanical treatment on microstructure and mechanical properties of blended elemental Ti-6Al-4V compacts," *Mater. Sci. Eng.*, vol. 102, no. 1, pp. 105–114, 1988, doi: 10.1016/0025-5416(88)90538-1.
[33] W. Ho, "Effect of omega phase on mechanical properties of Ti-Mo alloys for biomedical applications," *J. Med. Biol. Eng.*, vol. 28, no. 1, p. 47, 2008.
[34] H. Hsu, S. Wu, S. Hsu, W. Kao, and W. Ho, "Materials Science & Engineering A Structure and mechanical properties of as-cast Ti – 5Nb-based alloy with Mo addition," *Mater. Sci. Eng. A*, vol. 579, pp. 86–91, 2013, doi: 10.1016/j.msea.2013.05.004.
[35] D. J. Lin, J. H. Chern Lin, and C. P. Ju, "Structure and properties of Ti-7.5Mo-xFe alloys," *Biomaterials*, vol. 23, no. 8, pp. 1723–1730, 2002, doi: 10.1016/S0142-9612(01)00233-2.
[36] C. L. J. Lee CM, Ju CP, "Structure-property relstionship of cast Ti-Nb alloys," *J. oral rahabilitation*, 2002, doi: https://doi.org/10.1046/j.1365-2842.2002.00825.x.
[37] A. Panigrahi, "DISSERTATION / DOCTORAL THESIS „ Mechanical properties and phase transformation of severe plastic deformation "," pp. 1–116, 2016.
[38] H. Hsu, S. Wu, S. Hsu, J. Syu, and W. Ho, "Materials Science & Engineering A The structure and mechanical properties of as-cast Ti – 25Nb – x Sn alloys for biomedical applications," *Mater. Sci. Eng. A*, vol. 568, pp. 1–7, 2013, doi: 10.1016/j.msea.2013.01.002.